Nano-Infiltration for Enhancing Microwave Attenuation in Polystyrene-Nanoparticle Composites

Jagadeshvaran P. L.[1#], Harsha Nallabothula [1#], Aishwarya V. Menon[2] and Suryasarathi Bose[1]*

[1]*Department of Materials Engineering, Indian Institute of Science, Bangalore – 560012, India.*

[2]*Centre for Nanoscience and Engineering, Indian Institute of Science, Bangalore – 560012, India.*

**corresponding author email: sbose@iisc.ac.in ; Tel: +91-80-2293 3407*

#J and H have equally contributed to this work

Supporting Information

S1. Characterization of synthesized particles

Materials that consist of magnetic and electric dipoles are said to absorb the EM radiation and reduce EM pollution as compared to conducting particles that tend to reflect the EM radiation leading to cross-talk with any unshielded device. The shielding efficiency of these particles increases significantly when they are decorated onto a conducting network.

S1.1 Fe_3O_4 nanoparticles

Ferrite (Fe_3O_4) nanoparticles were synthesized through the co-precipitation method and used as EM absorbing materials in this study. The morphology of the synthesized ferrite particles was characterized through high magnification bright-field TEM techniques presented in Fig.S1(a). Fig.S1(a) confirm spherical morphology with the size around 10 nm. The crystal structures of the synthesized ferrite were analyzed through X-ray diffraction. In Fig.S1(b) the XRD pattern confirms the spinel structure of the ferrite particles and the peaks (220), (400), (422), (511), (440) and (533) were identified and matched with the peaks of fcc lattice as reported in the literature (JCPDS no. 88-0866). Magnetization behavior of Fe_3O_4 was characterized through room temperature VSM. From Fig.S1(c) the saturation magnetization was obtained to be 54.15 emu/g depicting strong magnetization characteristics.[27]

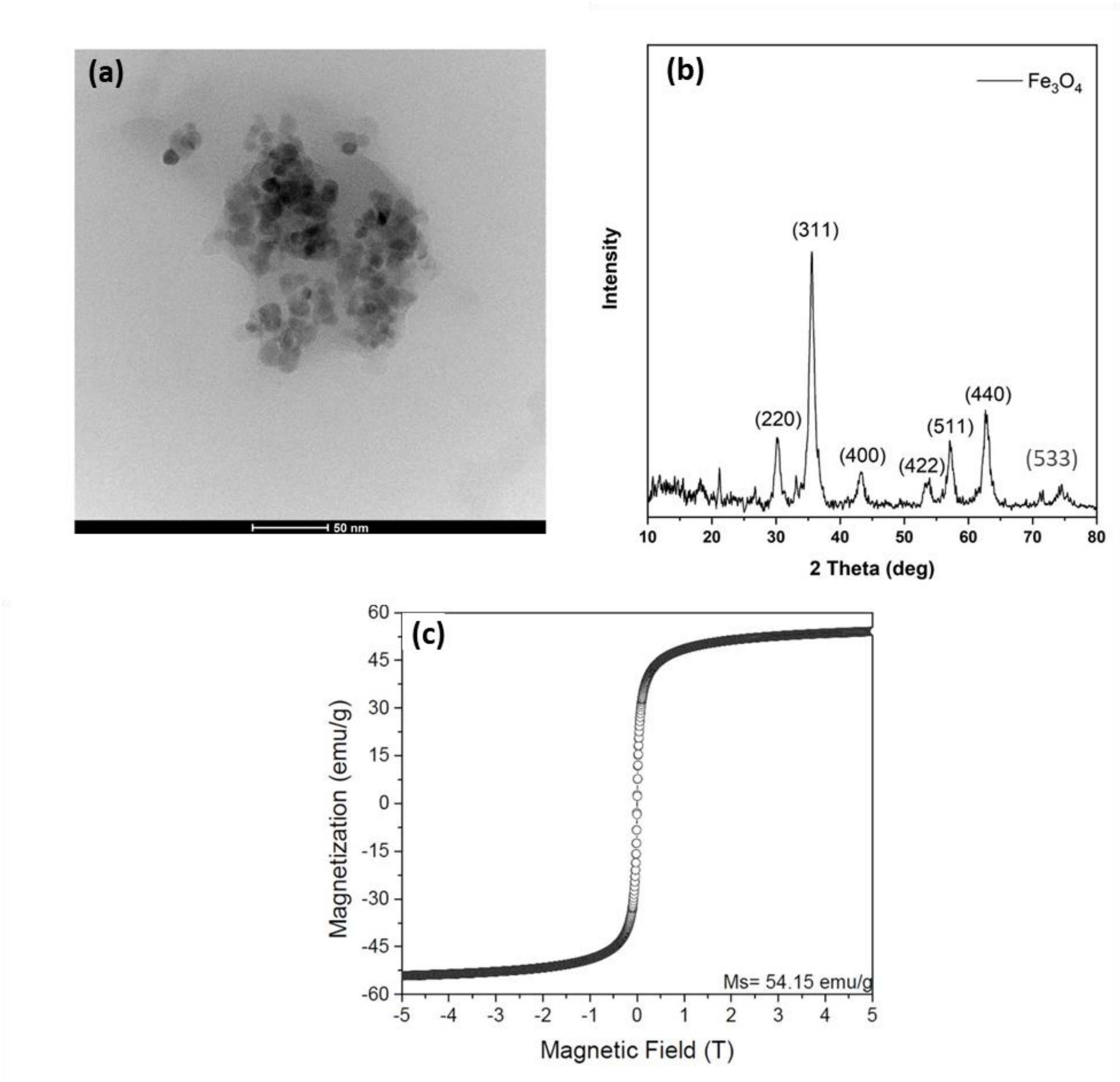

Fig.S1: Characterization of Fe_3O_4 nanoparticles. (a) TEM micrographs show that the size of particles is around 10 nm. (b) Powder XRD pattern of Fe_3O_4 nanoparticles confirms the material to be Fe_3O_4. (c) Room temperature VSM determined the magnetic hysterics and saturation magnetization.

S1.2 rGO-Fe_3O_4 nanoparticles

Fe_3O_4 decorated reduced Graphene oxide was synthesized through a one-pot hydrothermal method. From Fig.S2(a) the peaks in XRD pattern match the peaks of Fe_3O_4 indicating the presence of Fe_3O_4 as the peaks (220), (400), (422), (511), (440) and (533) were identified and matched with the peaks of fcc lattice as reported in the literature(JCPDS no. 88-0866). Magnetization behavior of rGO-Fe_3O_4 was characterized through room temperature VSM. From Fig.S2(b) and the saturation magnetization was obtained to be 21.2 emu/g.[30] The morphology of rGO-Fe_3O_4 particles was characterized through low and high magnification bright-field TEM techniques shown in Fig.S2(c). Fig. S2(c) shows Fe_3O_4 decorated on reduced Graphene oxide with a size of 10 nm.

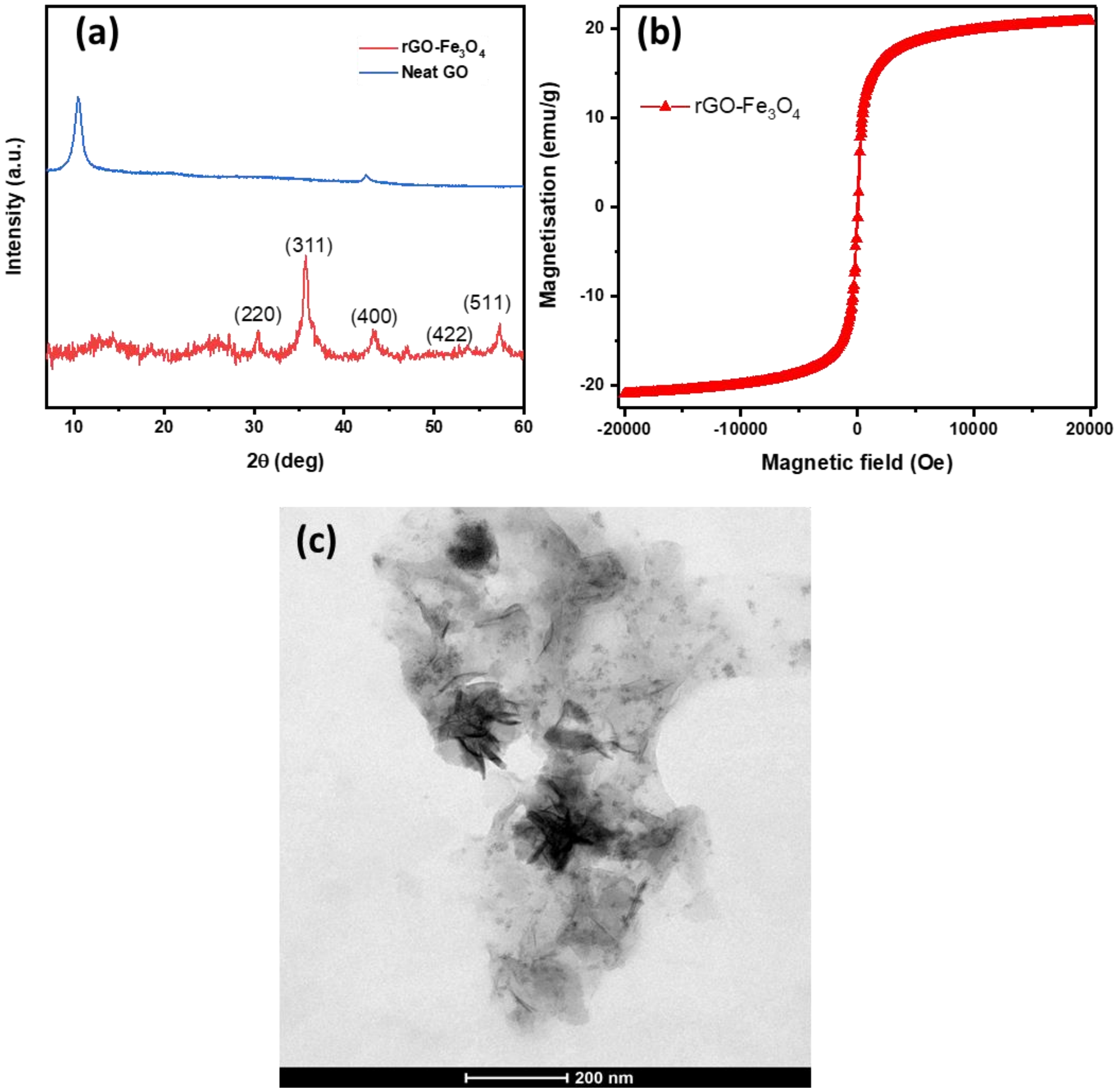

Fig.S2: Characterization of Fe_3O_4 nanoparticles. (a) Powder XRD pattern of rGO-Fe_3O_4 confirms the material to be Fe_3O_4. (b) Room temperature VSM determined the magnetic hysterics and saturation magnetization. (c) TEM micrographs show that the size of particles is around 10 nm decorated on reduced graphene

S1.3 rGO-MoS_2 nanoparticles

MoS_2 decorated reduced Graphene oxide was synthesized through a one-pot hydrothermal method. The morphology of rGO-MoS_2 particles was characterized through low and high magnification darkfield TEM shown in Fig.S3(a) and (b). Fig.3(a) describes the flower-like morphology of MoS_2 on reduced Graphene oxide with size varying between 200 nm and 400 nm and the polycrystallinity of from Fig.3(b).X-ray diffraction studies were also performed to confirm the structure. From Fig.S3(c) the peaks in the XRD pattern match the peaks of MoS_2 indicating the presence of MoS_2.

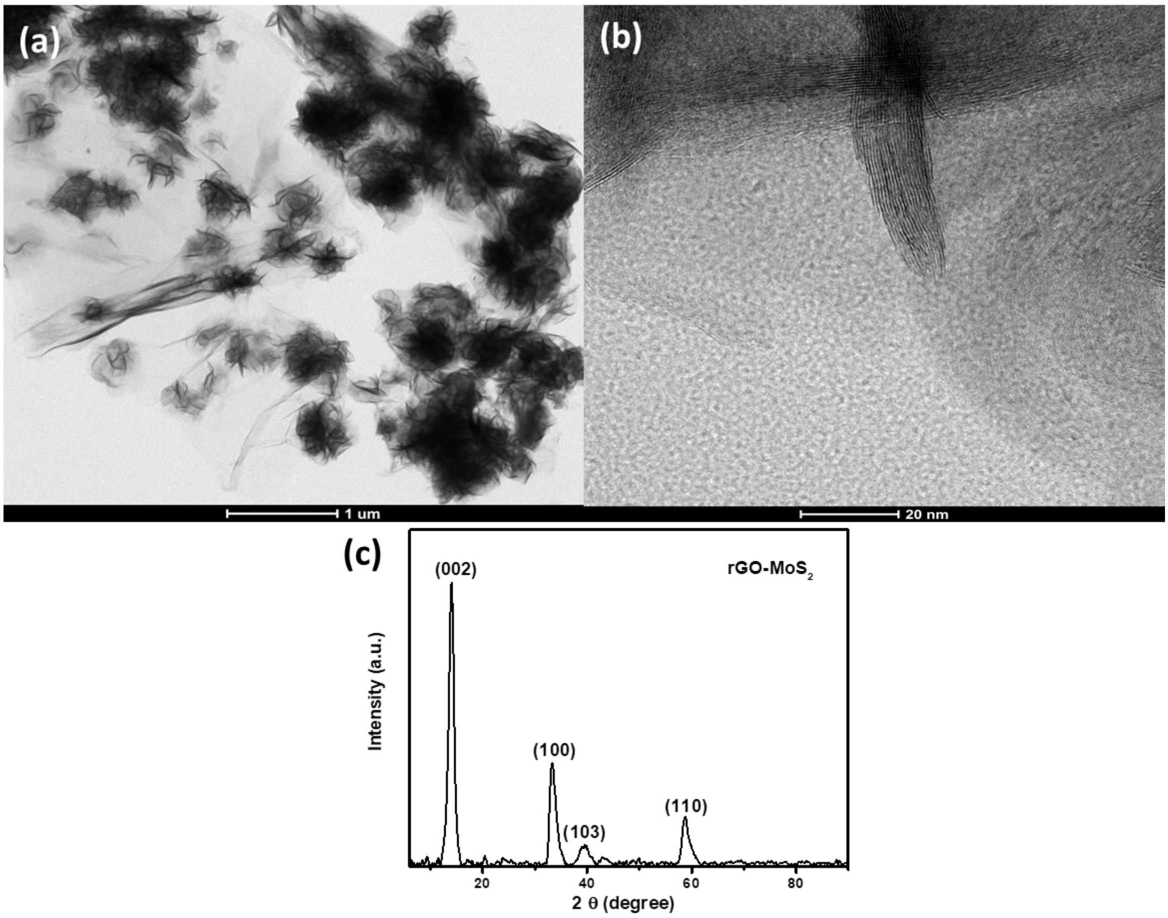

Fig.S3: Characterization of rGO-MoS_2. (a) TEM micrograph describing the morphology and dimensions of MoS_2 decorated on reduced Graphene oxide (b) shows the polycrystallinity of the material. (c) Powder XRD pattern confirms the material to be rGO-MoS_2

S2. Digital images of the composites subjected to nano-infiltration

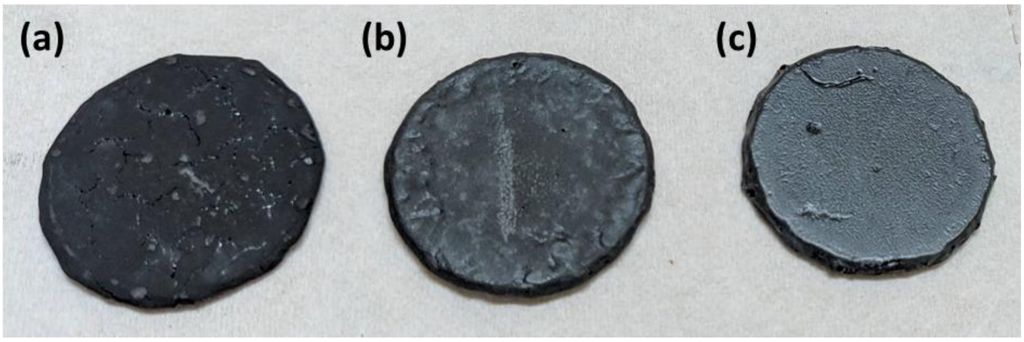

Figure S4: Digital images of solvent-induced infiltration into PS- 5 wt% MWCNT (a)rGO-MoS_2 (3 layers), (b) single layer rGO-MoS_2 and (c) single layer of rGO-Fe_3O_4. With the increase in the number of layers the lustrous texture of the surface is lost which indicates poor infiltration of filler material.

S3. EMI shielding measurements of preliminary samples

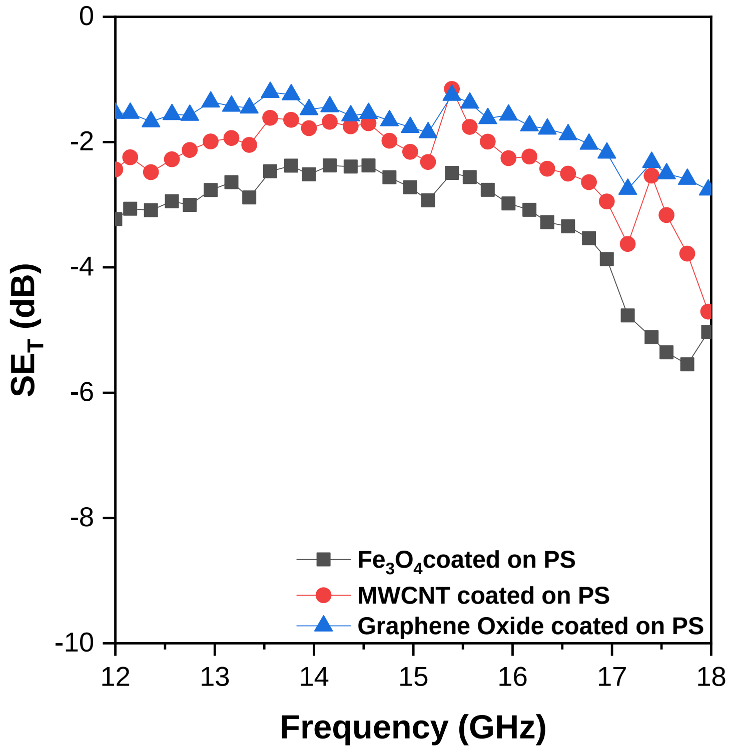

Figure S5: Total shielding effectiveness of Fe_3O_4, MWCNT, and graphene oxide coated polystyrene composites

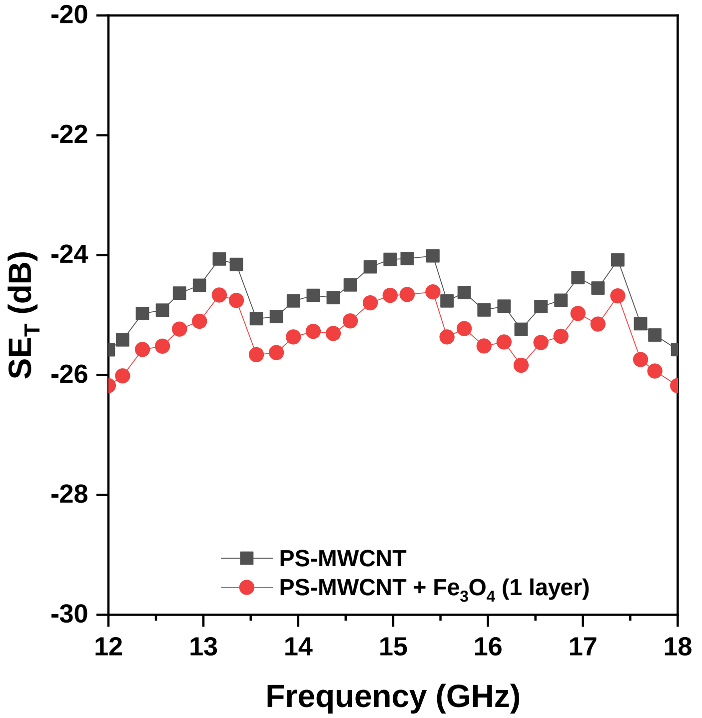

Figure S6: Total shielding effectiveness of Fe_3O_4 coated on PS- MWCNT in comparison to PS- MWCNT composites. The presence of Fe_3O_4 has improved the shielding effectiveness by a small amount.